



Influence of fiber-matrix interphase on high temperature behavior of glass-ceramic matrix composites
by Ramazan Kahraman

A thesis submitted in partial fulfillment of the requirements for the degree of Doctor of Philosophy in
Chemical Engineering

Montana State University

© Copyright by Ramazan Kahraman (1993)

Abstract:

The influence of the fiber-matrix interphase on the high temperature behavior of Nicalon fiber reinforced CAS-II glass-ceramic matrix composites has been investigated. Unidirectional and cross-ply laminates were studied from 20° up to 1000°C. Tensile testing at 1000°C in air lowered the longitudinal unidirectional strength to the stress level at which matrix cracking began to occur. Interfaces exposed along matrix cracks increased in bond strength, resulting in brittle composite fracture. The strength of crossplied composites was also severely reduced in 800°C air. Transverse plies cracked prior to 0° ply matrix cracking. However, embrittlement did not occur until the matrix in the 0° plies cracked.

Interphase oxidation did not appear to play a significant role in crack growth parallel to the fibers of transverse plies except near exposed edges. Oxygen did not appear to have penetrated the transverse cracks except directly on the specimen fracture surface. This was evidenced by a lack of bond strength changes along the transverse ply cracks. The surprising lack of apparent oxidation effects on 90° ply cracking led to further investigation of crack growth parallel to the fibers using the double torsion test to measure the transverse fracture toughness (G_{Ic}) of unidirectional materials, and to look for evidence of environmental stress cracking. G_{Ic} did decrease moderately with increasing temperature (as does the bulk matrix), but no evidence of an interphase oxidizing effect on crack growth could be found. Cracks would not grow in the oxidizing environment at G_I values slightly below G_{Ic} , and oxidation did not occur on the part of the fracture surface which was cracked but not widely opened during the test.

The results of this study establish that oxidation does not take part in crack growth parallel to the fibers, except adjacent to exposed edges. Neither does oxygen enter 90° ply cracks in crossplied composites in sufficient quantity to produce oxidation embrittlement, at least up to the 0° matrix cracking strain. Matrix cracks in the 0° plies at higher strains do allow oxidation embrittlement of the 0° plies in unidirectional and crossplied composites. Contacts between fibers and matrix along the 90° ply cracks may locally seal-off and prevent further spread of oxygen. No such contacts and possible sealing-off occur along matrix cracks in the 0° plies, and oxygen is free to spread throughout the opened matrix crack to reach the carbon interphase regions.

INFLUENCE OF FIBER-MATRIX INTERPHASE ON HIGH TEMPERATURE
BEHAVIOR OF GLASS-CERAMIC MATRIX COMPOSITES.

by

Ramazan Kahraman

A thesis submitted in partial fulfillment
of the requirements for the degree

of

Doctor of Philosophy

in

Chemical Engineering

MONTANA STATE UNIVERSITY
Bozeman, Montana

February 1993

D378
K1225

APPROVAL

of a thesis submitted by

Ramazan Kahraman

This thesis has been read by each member of the thesis committee and has been found to be satisfactory regarding content, English usage, format, citations, bibliographic style, and consistency, and is ready for submission to the College of Graduate Studies.

2/8/93
Date

John D. Mandell
Co-chairperson, Graduate Committee

2/8/93
Date

Mark C. Decker
Co-chairperson, Graduate Committee

Approved for the Major Department

2/8/93
Date

John T. Lewis
Head, Major Department

Approved for the College of Graduate Studies

2/10/93
Date

Ed Brown
Graduate Dean

STATEMENT OF PERMISSION TO USE

In presenting this thesis in partial fulfillment of the requirements for a doctoral degree at Montana State University, I agree that the Library shall make it available to borrowers under rules of the Library. I further agree that copying of this thesis is allowable only for scholarly purposes, consistent with "fair use" as prescribed in the U.S. Copyright Law. Requests for extensive copying or reproduction of this thesis should be referred to University Microfilms International, 300 North Zeeb Road, Ann Arbor, Michigan 48106, to whom I have granted "the exclusive right to reproduce and distribute copies of the dissertation in and from microfilm and the right to reproduce and distribute by abstract in any format."

Signature  _____Date 2. 8. 1993

Dedicated to my mother, Hatice Sümer

ACKNOWLEDGEMENTS

I am grateful to Prof. John F. Mandell for providing unending guidance and enlightenment throughout the course of this research. I am also thankful to Prof. Max C. Deibert for his continuous encouragement and support. Especially, his help in my learning the writing skills is greatly appreciated.

I wish to thank the remaining members of my thesis committee, Prof. John T. Sears, Prof. Bonnie Tyler, Prof. Aleksandra Vinogradov and Prof. Earl Skogley, for their support and contributions. The contributions of Prof. Robert L. Nickelson and Prof. Ronald W. Larsen are also appreciated.

The faculty and staff of the Chemical Engineering Department have created a very pleasant working environment. I wish to express my special thanks to the secretaries, Jane Curtis, Margie Jenson and Monica Hoey, who helped me work with the system, always with a smile.

The contributions of my fellow graduate students are highly valued. Although many have contributed in some small way, the larger contributions of James B. Schutz and Skyh-Hua Jao (during his study at Massachusetts Institute of Technology) are most gratefully acknowledged.

This research would not have occurred without the composite materials supplied by Corning, Inc., their help is also acknowledged. I also wish to acknowledge the donation of high temperature testing equipment by Instron Corp.

The unending support of my family is gratefully appreciated. Thanks to my parents for their unending moral support and understanding. Finally, thanks to my wife, Sibel, for her sacrifices and patience throughout this work. I also feel sorry for and apologize to my little daughter, Betül, for not going home to be with her when she had called me and said "come home daddy" almost every day during the last year of this study.

TABLE OF CONTENTS

	Page
APPROVAL	ii
STATEMENT OF PERMISSION TO USE	iii
ACKNOWLEDGEMENTS	v
TABLE OF CONTENTS	vi
LIST OF TABLES	ix
LIST OF FIGURES	x
ABSTRACT	xvi
INTRODUCTION	1
BACKGROUND	3
Mechanical Behavior of Ceramic Matrix Composites	3
Longitudinal Tensile Strength	3
Longitudinal Toughness	9
Transverse Properties	10
Interface (or Interphase) Effects on Composite Properties	11
Interphase in Nicalon Reinforced Glass-Ceramics	13
Environmental Effects.....	15
Test Methods to Determine Tensile Properties of Ceramic Matrix Composites	19
Review of Fracture Mechanics Concepts	23
Fracture Test Methods for Ceramic Matrix Composites	26
The Double Torsion Test	30

TABLE OF CONTENTS--Continued

	Page
Methods for Determining Interfacial Properties in Ceramic Matrix Composites	35
Microscopy Techniques	38
EXPERIMENTAL	42
Materials	42
Tensile Testing	43
Equipment	43
Specimen Design	48
Test Procedure	49
Determination of the Transverse Fracture Toughness by Double Torsion Technique	51
Equipment	51
Specimen Preparation and Test Procedure	55
Microdebonding Test Method	61
Test Apparatus	61
Specimen Preparation	64
Test Procedure and Analysis	66
Scanning Electron Microscopy	72
Test System	72
Specimen Preparation	72
RESULTS AND DISCUSSION	74
Tensile Behavior	75
Tests on Unidirectional Nicalon/CAS-II	76
Behavior of Crossplied Laminates	98
Transverse Fracture Toughness Test Results	116

TABLE OF CONTENTS--Continued

	Page
Compliance Calibration	116
Room Temperature Test Results	118
High Temperature Transverse Fracture Results	127
CONCLUSIONS	156
RECOMMENDATIONS	160
REFERENCES	162
APPENDICES	170
Appendix A - Mechanical Properties of Nicalon/CAS-II Composite	171
Appendix B - Reliability of the Double Torsion Test Results	173
Repeatability of the Double Torsion Test Results	188
Double Torsion Tests Performed on Glass Specimens	189
Appendix C - Example Data of a Microdebonding Test ..	195
Appendix D - Tensile Test Data	197
Appendix E - Composite Plate Designations	199
Appendix F - Auger Electron Spectroscopy Analysis ...	201
Appendix G - Analytical Compliance Calibration for DT Tests on Soda-Glass Specimens	205
Analytical Compliance Calibration for Nicalon/CAS-II DT Specimens	206

LIST OF TABLES

Table	Page
1. Transverse penetration of oxidation for Nicalon/CAS-II composite upon exposure to air at 1000°C for several exposure times	92
2. Fiber-matrix bond strength measurements on Nicalon/CAS-II samples, exposed to air at 1000°C for several exposure times, at various depths below the exposed surface	145
3. Mechanical properties of Nicalon/CAS-II composite	172
4. Repeatability of the compliance calibration results of the double torsion tests performed on a steel specimen	189
5. Microdebonding test results for a unidirectional Nicalon/CAS-II sample from plate 1, as received ..	196
6. Tensile test data on unidirectional and crossplied Nicalon/CAS-II composites	198
7. Nicalon/CAS-II composite plate designations	200

LIST OF FIGURES

Figure	Page
1. Failure processes in ceramic matrix composites ...	4
2. Model tensile stress-strain behavior for fiber reinforced ceramic matrix composites	6
3. Dependence of composite strength on fiber content	7
4. Interface dominated properties	12
5. Effect of fiber strength and interfacial shear strength on fracture mechanism for ceramic matrix composites	17
6. Double torsion test configuration	31
7. A schematic of loading for the microdebonding test	39
8. Photograph of the mechanical testing system	45
9. Loading section of the tensile testing system while the furnace is in use	46
10. Photograph of the high temperature extensometer and its attachment to the tensile specimen	47
11. Tensile test specimen configuration	50
12. Loading section of the double torsion test system	53
13. Double torsion test fixture	54
14. Specimen compliance calibration load vs. displacement plot	56
15. Double torsion specimen for fracture testing, including notch root detail	58
16. Specimen load vs. displacement plot from the double torsion tests to failure	59

LIST OF FIGURES--Continued

	Page
17. Microdebonding test system	62
18. The microscope and microindentation station of the microdebonding test system	63
19. The probe for the microdebonding test system	65
20. Polished and debonded Nicalon/CAS-II surfaces	67
21. Finite element model used for microdebonding analysis	70
22. Representative room temperature longitudinal tensile stress-strain curve for unidirectional Nicalon/CAS-II composite	77
23. Polished edge of a unidirectional Nicalon/CAS-II tensile specimen fractured at room temperature....	80
24. Fiber-matrix debonding prior to crack propagation	81
25. Fracture surface of a unidirectional Nicalon/ CAS-II tensile specimen tested at room temperature	82
26. Tensile stress-strain curves of unidirectional Nicalon/CAS-II composites at different temperatures	84
27. Fracture surface of a unidirectional Nicalon/ CAS-II tensile specimen tested in air at 1000°C with a rate of 0.7% strain/h	86
28. Matrix crack extending through the fibers	88
29. Fracture surface of a unidirectional Nicalon/ CAS-II tensile specimen tested in air at 1000°C with a rate of 0.7% strain/min	89
30. Diagram showing sample exposed to air at 1000°C to determine the transverse oxidation penetration for several exposure times	91
31. Ultimate tensile strain at temperature for Nicalon fiber and unidirectional Nicalon/CAS-II composite	94

LIST OF FIGURES--Continued

	Page
32. Normalized tensile strength at temperature for Nicalon fiber and unidirectional Nicalon/CAS-II composite	95
33. Representative room temperature tensile stress-strain curve for cross-ply Nicalon/CAS-II composite	99
34. Polished edge of a cross-ply Nicalon/CAS-II tensile specimen fractured at room temperature ...	102
35. A crack in a cross-ply Nicalon/CAS-II tensile specimen tested at room temperature	103
36. Tensile stress-strain curves of cross-ply Nicalon/CAS-II composites at different temperatures	105
37. Fracture surface of a cross-ply Nicalon/CAS-II tensile specimen tested in air at 800°C with a rate of 0.7% strain/h	106
38. Fracture surface of a cross-ply Nicalon/CAS-II tensile specimen tested at room temperature	107
39. Fracture surface of a cross-ply Nicalon/CAS-II tensile specimen tested in air at 800°C with a rate of 0.7% strain/min	109
40. Fracture surface close to an edge of a cross-ply Nicalon/CAS-II tensile specimen tested in air at 800°C with a rate of 0.7% strain/min	110
41. Diagram showing a cross-ply composite tensile specimen	112
42. Polished edge of a cross-ply Nicalon/CAS-II tensile specimen fractured at 800°C	113
43. A crack at a depth of about 0.5 mm below an edge of a cross-ply Nicalon/CAS-II tensile specimen fractured at 800°C	114
44. Compliance vs. crack length plot for Nicalon/CAS-II double torsion specimens	117

LIST OF FIGURES--Continued

	Page
45. Double ramp on a composite double torsion specimen for initiation of a sharp crack at the notch tip	120
46. Notch tip on the lower face of a Nicalon/CAS-II double torsion specimen before loading	121
47. Notch tip on the lower face of a Nicalon/CAS-II double torsion specimen after loading to about 85% of the critical load	122
48. Fracture surface of a Nicalon/CAS-II double torsion specimen tested at room temperature	124
49. SEM micrograph of a fracture surface of a Nicalon/CAS-II double torsion specimen tested at room temperature	125
50. Room temperature transverse fracture toughness vs. crack length for Nicalon/CAS-II double torsion specimens	126
51. Load vs. displacement plots of double ramps on an inconel rod at 800°C with different ramp rates ...	128
52. Transverse fracture toughness vs. temperature plot for Nicalon/CAS-II specimens fractured in 2-3 min	131
53. Transverse fracture toughness vs. temperature plot for Nicalon/CAS-II specimens fractured in 9-10 h	132
54. Transverse fracture toughness vs. temperature plot for Nicalon/CAS-II specimens fractured in 1-2 h	133
55. Transverse fracture toughness vs. time to failure plot of Nicalon/CAS-II composite	134
56. Fracture surface of a Nicalon/CAS-II double torsion specimen tested at 1000°C with a rate of 22 N/h	136

LIST OF FIGURES--Continued

	Page
57. SEM micrograph taken on the planar part in the first half of the fracture surface of a Nicalon/CAS-II double torsion specimen tested at 1000°C with a rate of 22 N/h	137
58. Close-up of the fracture surface in Figure 57	138
59. SEM picture taken near the end of the fracture surface of a Nicalon/CAS-II double torsion specimen tested at 1000°C at a rate of 22 N/h	139
60. Close-up of the fracture surface in Figure 59	140
61. SEM micrograph taken on the rough part in the second half of the fracture surface of a Nicalon/CAS-II double torsion specimen tested at 1000°C with a rate of 22 N/h	141
62. Diagram showing composite specimen fractured in air at 1000°C (22 N/h), indicating where the data in Figure 63 were taken	142
63. Fiber-matrix bond strength vs. depth below the exposed surface for a Nicalon/CAS-II sample oxidized at 1000°C for 10 h	144
64. Fracture surface of a Nicalon/CAS-II double torsion specimen tested at 1000°C with a displacement rate of 0.1 mm/h	147
65. Cross-section of a Nicalon/CAS-II double torsion specimen fractured at 800°C	149
66. Interfacial bond strength distribution along the crack from the top to the bottom surface for Nicalon/CAS-II double torsion specimens fractured at different temperatures	150
67. Diagram showing the contacts between fibers and matrix along the fiber axis as the fibers are slightly extracted from the matrix	154
68. Load vs. displacement plot of a double torsion test performed on steel	175

LIST OF FIGURES--Continued

	Page
69. Load vs. displacement plot of a double torsion test performed on steel after previously ramping to a displacement of 0.02 mm	176
70. Load vs. displacement plot of a double torsion test performed on steel without using the adjustment rods in the test fixture	178
71. Load vs. displacement plot of a double ramp on a steel ball bearing	179
72. Load vs. displacement plot of a double ramp on the loading rod clamped in the lower grip	181
73. Load vs. displacement plot of a double ramp on the loading rod, as load measured by the higher capacity load cell	182
74. Load vs. displacement plot of a double ramp on a metal rod clamped in the grips	183
75. Compliance calibration load vs. displacement plot of a double torsion test on glass	184
76. Double torsion test system including the extensometer used for measuring the load-point displacement	186
77. Load vs. displacement plot of a double ramp on Nicalon/CAS-II where displacement was measured through both the actuator and the extensometer....	187
78. Compliance vs. crack length plot for glass double torsion specimens	191
79. Load vs. displacement plot of a double torsion test to failure on a glass specimen	192
80. Fracture toughness vs. crack length plot for glass double torsion specimens	193
81. AES depth profile conducted on a fiber from Nicalon/CAS-II fracture surface	203

ABSTRACT

The influence of the fiber-matrix interphase on the high temperature behavior of Nicalon fiber reinforced CAS-II glass-ceramic matrix composites has been investigated. Unidirectional and cross-ply laminates were studied from 20° up to 1000°C. Tensile testing at 1000°C in air lowered the longitudinal unidirectional strength to the stress level at which matrix cracking began to occur. Interfaces exposed along matrix cracks increased in bond strength, resulting in brittle composite fracture. The strength of crossplied composites was also severely reduced in 800°C air. Transverse plies cracked prior to 0° ply matrix cracking. However, embrittlement did not occur until the matrix in the 0° plies cracked.

Interphase oxidation did not appear to play a significant role in crack growth parallel to the fibers of transverse plies except near exposed edges. Oxygen did not appear to have penetrated the transverse cracks except directly on the specimen fracture surface. This was evidenced by a lack of bond strength changes along the transverse ply cracks. The surprising lack of apparent oxidation effects on 90° ply cracking led to further investigation of crack growth parallel to the fibers using the double torsion test to measure the transverse fracture toughness (G_{Ic}) of unidirectional materials, and to look for evidence of environmental stress cracking. G_{Ic} did decrease moderately with increasing temperature (as does the bulk matrix), but no evidence of an interphase oxidizing effect on crack growth could be found. Cracks would not grow in the oxidizing environment at G_I values slightly below G_{Ic} , and oxidation did not occur on the part of the fracture surface which was cracked but not widely opened during the test.

The results of this study establish that oxidation does not take part in crack growth parallel to the fibers, except adjacent to exposed edges. Neither does oxygen enter 90° ply cracks in crossplied composites in sufficient quantity to produce oxidation embrittlement, at least up to the 0° matrix cracking strain. Matrix cracks in the 0° plies at higher strains do allow oxidation embrittlement of the 0° plies in unidirectional and crossplied composites. Contacts between fibers and matrix along the 90° ply cracks may locally seal-off and prevent further spread of oxygen. No such contacts and possible sealing-off occur along matrix cracks in the 0° plies, and oxygen is free to spread throughout the opened matrix crack to reach the carbon interphase regions.

INTRODUCTION

Glass-ceramic materials are ceramics produced by the controlled crystallization of appropriate glasses [1]. When these materials are fabricated, they are processed as glasses (while the materials are in a viscous form), then crystallized under controlled heat treatment conditions to achieve materials with superior toughness and high temperature strength [2]. They consist of a large proportion, typically 95 to 98 volume percent, of very small crystals, generally smaller than 1 micron, with a small amount of residual glass (amorphous) phase to make up a pore-free ceramic [1].

The recent development of ceramic or glass-ceramic matrix composites has been driven primarily by the need for high temperature structural materials for applications such as heat engines and space planes. While monolithic structural ceramics and glass-ceramics are also being developed to meet these needs, they have problems in structural applications due to their inherent brittleness. Glass-ceramic matrix composites offer potential to achieve high performance at high temperatures [3]. Considerable attention has been focused on (continuous or relatively long) fiber-reinforced glass-ceramics. The fiber addition increases toughness through crack deflection and fiber bridging behind the crack tip [3,4].

Ceramic matrix composites do not simply consist of a combination of reinforcement and matrix phases. More typically, either through fiber precoating or through reactions during processing, the resultant composites contain an interphase region separating the reinforcement and matrix phases that is very important in controlling the properties of the composite. Chemical compositions and processing conditions have a strong influence on the thickness of this interphase [3,5]. The main objective of this research was to develop a better understanding of the influence of the fiber-matrix interphase on high temperature behavior of multidirectional glass-ceramic matrix composites under the oxidizing conditions which exist in most potential applications.

BACKGROUND

Ceramic and glass-ceramic composites offer a great range of utility both on a high temperature basis as well as on other environmental considerations such as oxidation resistance, erosion, and chemical attack from acids, etc. [2,6]. The properties of these composites depend on the combination of the properties of starting materials and the fabrication procedure [3]. The fibers should not be greatly degraded during processing either by handling or by chemical reaction. Also, the resultant fiber-matrix interphase must have the characteristics necessary for optimum composite properties, as will be discussed in the following sections.

Mechanical Behavior of Ceramic Matrix Composites

Longitudinal Tensile Strength

In ceramic matrix composites (CMC's), the matrix failure strains are generally less than the fiber breaking strains [7,8,9]. The lower matrix failure strain indicates matrix failure prior to fiber failure. The possible failure modes for unidirectional CMC's are depicted in Figure 1 [10]. For strongly bonded systems, cracks formed in the matrix propagate through the interphase and the fibers without causing fiber-

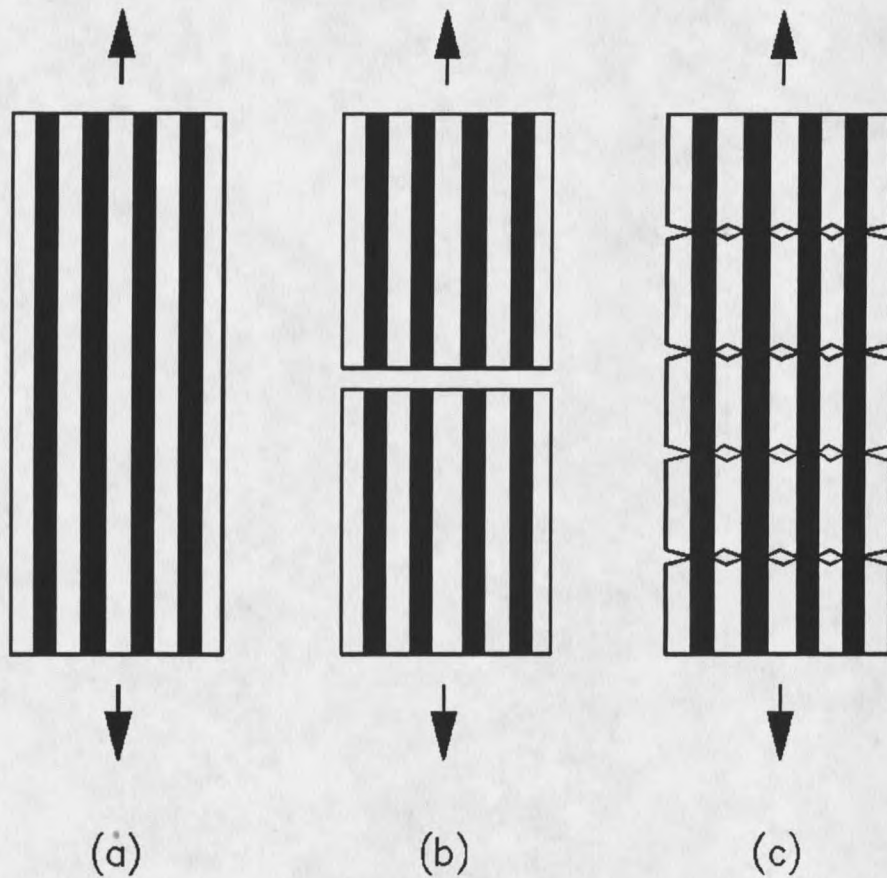


Figure 1. Failure processes in ceramic composites [10]: (a) before fracture; (b) simultaneous matrix and fiber fracture in a strongly bonded system; (c) multiple matrix cracking and fiber debonding prior to fiber failure in a weakly bonded system

matrix debonding as shown in Figure 1b [11]. Composite failure occurs at the matrix failure strain (ϵ_{mu}) by propagation of a single crack through the fibers. A linear stress-strain curve (Figure 2a) results due to the brittle nature of the fracture. Composite longitudinal strength (σ_{cL}) and modulus (E_{cL}) are expressed by the rule of mixtures [12]:

$$\sigma_{cL} = E_{cL} \epsilon_{mu} \quad (2)$$

$$E_{cL} = E_f V_f + E_m V_m \quad (1)$$

where E_f : fiber modulus

V_f : fiber volume fraction

E_m : matrix modulus

V_m : matrix volume fraction ($1-V_f$)

Some strength enhancement is possible with high modulus fibers through the higher E_{cL} , but this is limited. The composite failure strain remains essentially unchanged from that of the unreinforced typically brittle matrix. In addition, longitudinal toughness (resistance to crack growth perpendicular to fibers due to a longitudinal stress) is not greatly enhanced over that of the matrix.

Stronger CMC's are possible in weakly bonded systems above a critical fiber volume fraction, V_{cr} . The dependence of composite strength on V_f is illustrated in Figure 3 [13]. If the fiber content is too low, the reinforcing fibers may be

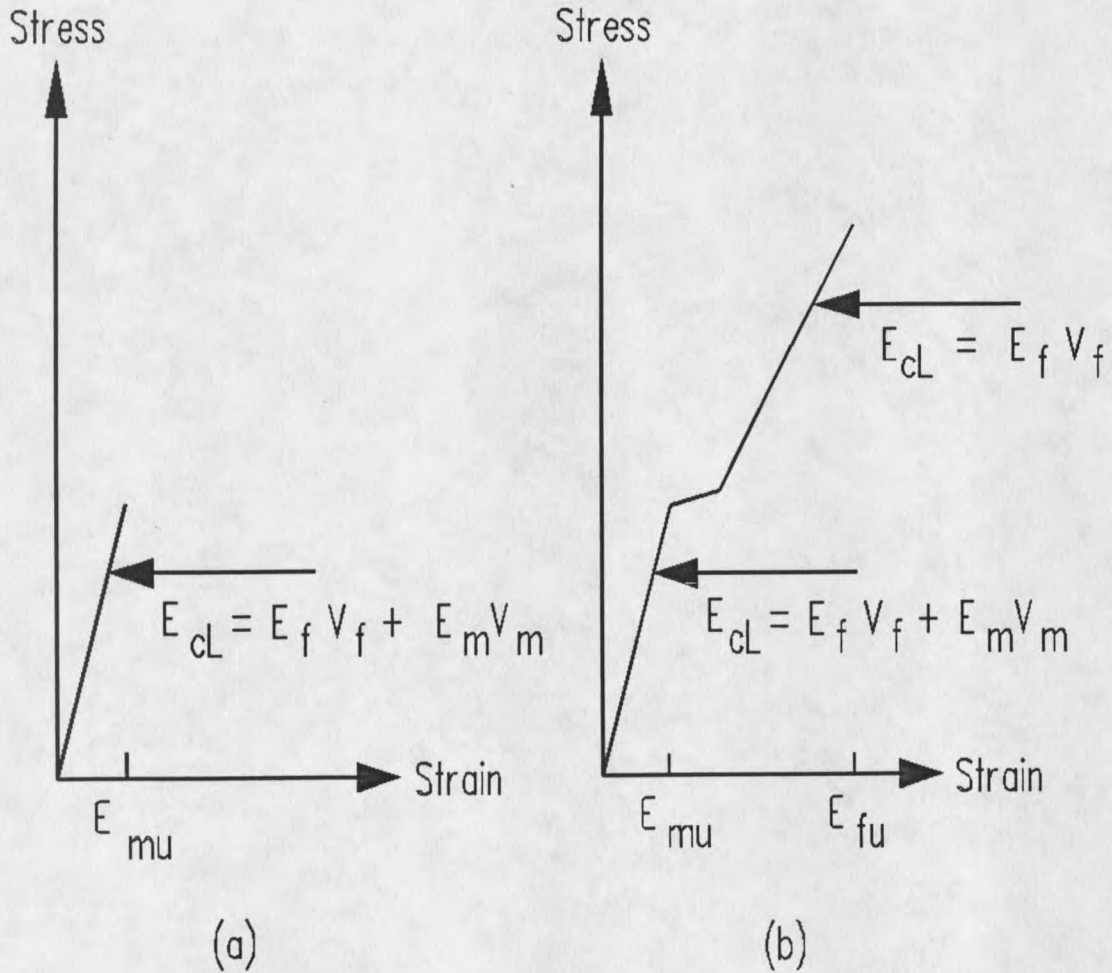


Figure 2. Model longitudinal tensile stress-strain behavior for fiber reinforced ceramic matrix composites [10]: (a) strongly bonded system; (b) weakly bonded system

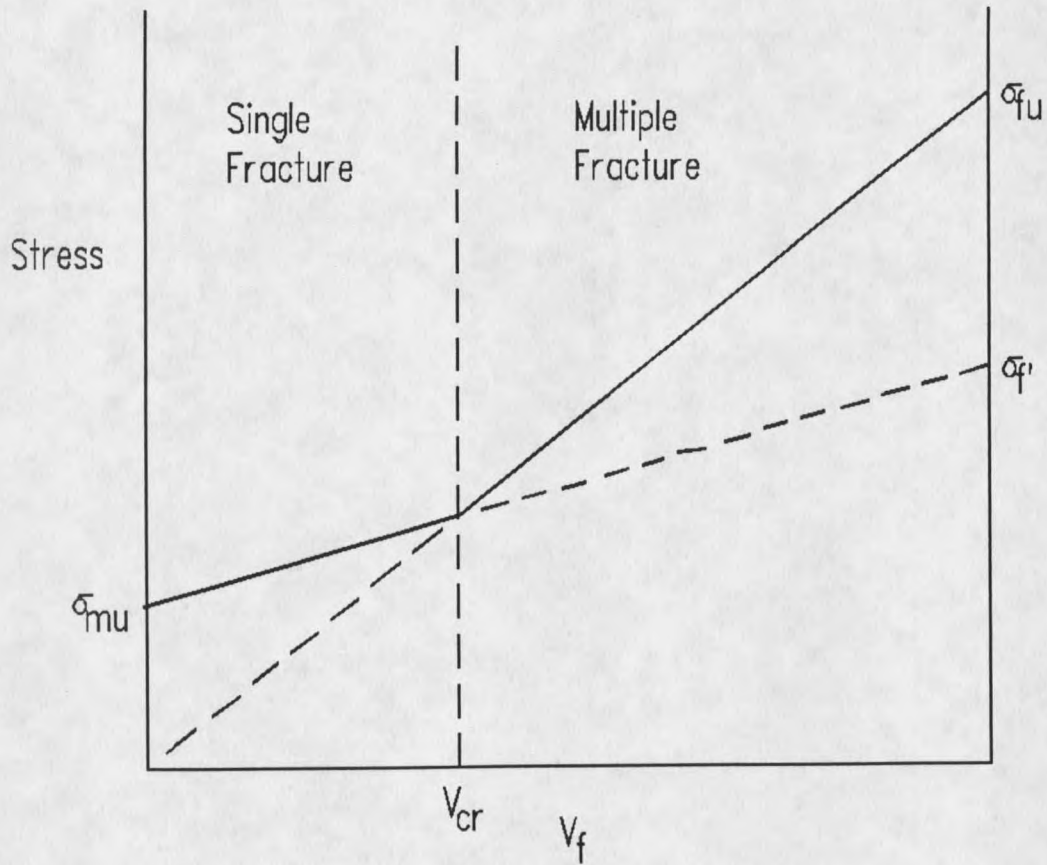


Figure 3. Dependence of composite strength on fiber content [13] (where σ_{mu} is matrix strength, σ_{fu} is fiber strength and σ_f is stress in the fiber at matrix fracture)

unable to support the total load carried by the composite when the matrix fails. Below V_{cr} , even in weakly bonded systems, composite strength is governed by the strength of the matrix. Failure occurs by single fracture, as described above.

Above V_{cr} , weakly bonded composites (Figure 1c) do not fail by the propagation of a single matrix crack [12,13,14]. The weak bond (or interphase) prevents spontaneous propagation of matrix cracks through adjacent fibers. After initial cracking of the matrix, the load is transferred to the fibers. The high fiber content allows support of the applied load, and multiple matrix cracking occurs with further stressing. The fiber volume fraction at the transition from single to multiple fracture is [12]:

$$V_{cr} = \frac{\sigma_{mu}}{\sigma_{mu} + \sigma_{fu} - \sigma_{f'}} \quad (3)$$

where σ_{mu} : matrix strength

σ_{fu} : fiber strength

$\sigma_{f'}$: stress in the fiber at matrix fracture

Matrix cracking, accompanied by load transfer to the fibers, can continue until a saturation crack density level is achieved. After matrix crack saturation, the fibers bear almost all of the load. Failure of the composite occurs when the fracture strength of the fibers is exceeded.

The stress-strain curve for weakly bonded composites is non-linear, consisting of three distinct regions as shown in Figure 2b [13]. In the initial linear portion of the curve, the composite stress and modulus are described by the rule of mixtures. A deviation from linearity occurs at the matrix microcracking strain. Further load increase beyond the onset of microcracking causes additional matrix cracking and a permanent decrease in composite stiffness due to a decreased matrix contribution. The final linear regime of the stress-strain curve is governed primarily by fiber properties. Failure of the ideal composite material occurs at an ultimate tensile strength approximated by the product of fiber strength and fiber volume fraction ($\sigma_{fu}V_f$). The ultimate composite failure strain, ϵ_{cu} , is increased over that of the unreinforced matrix and is (approximately) equivalent to that of the reinforcing fibers.

Longitudinal Toughness

The toughness (for cracks perpendicular to fibers) of CMC's cannot be expressed in terms of conventional fracture mechanics parameters (i.e. critical stress intensity factor) since failure does not occur by the growth of a single crack. While the toughness cannot be readily quantified, the resistance to notches and flaws is greatly increased if the fiber-matrix bond is weak, and then the behavior parallels

that of tough reinforced plastics [3,11]. If the interfacial bond is strong, the longitudinal toughness can be as low as that of the monolithic matrix, since a single planar crack grows through the fibers and matrix [5,11,12].

Transverse Properties

In most theoretical and experimental treatments of ceramic matrix composites, only the improvements in longitudinal properties over the monolithic matrix materials are highlighted. Little coverage is given to transverse properties of these composites. The transverse properties of uniaxially reinforced ceramics depend on the toughness of the matrix and interface directly, with little benefit of effects like fiber bridging, as will be discussed in the following section.

The poor transverse properties of some unidirectionally reinforced ceramics limit their use, since there are few engineering applications where transverse stresses are not encountered [10,14]. The resistance to crack growth parallel to the fibers is especially a determining factor for the useful design stress range since cracking parallel to the fibers is usually the initial form of damage in multidirectional composites [15]. This cracking process has been associated with the (transverse) fracture toughness, defined by the critical strain energy release rate, G_{Ic}

[16,17], which will be discussed in detail later.

Interface (or Interphase) Effects on Composite Properties

The fiber-matrix interphase plays a critical role in transferring loads in a composite. Figure 4 [11] illustrates three critical aspects of glass and ceramic matrix composite behavior which depend strongly on the interphase. The off-axis and shear properties (Figure 4a) such as shear strength, transverse tensile strength and transverse toughness are expected to correlate directly with fiber-matrix bond strength if other parameters remain unchanged [11,14].

Figures 4b and 4c illustrate the effect of the interphase on composite longitudinal toughness. As noted earlier, if the interphase is too strong, then, when matrix cracks form normal to the fibers, they can propagate through the fibers, giving brittle behavior similar to that in monolithic glasses and ceramics [5,11,12,18,19]. A sufficiently low fiber-matrix bond strength will increase flaw tolerance by allowing fiber debonding during crack propagation perpendicular to the fibers (fiber bridging) and/or by deflecting matrix cracks parallel to the fibers [3,11,12].

The pattern in glass and ceramic matrix systems without strong bonding of forming matrix cracks normal to the locally debonded fibers is indicated in Figure 4c. The stress at which significant matrix cracks form in unidirectional specimens

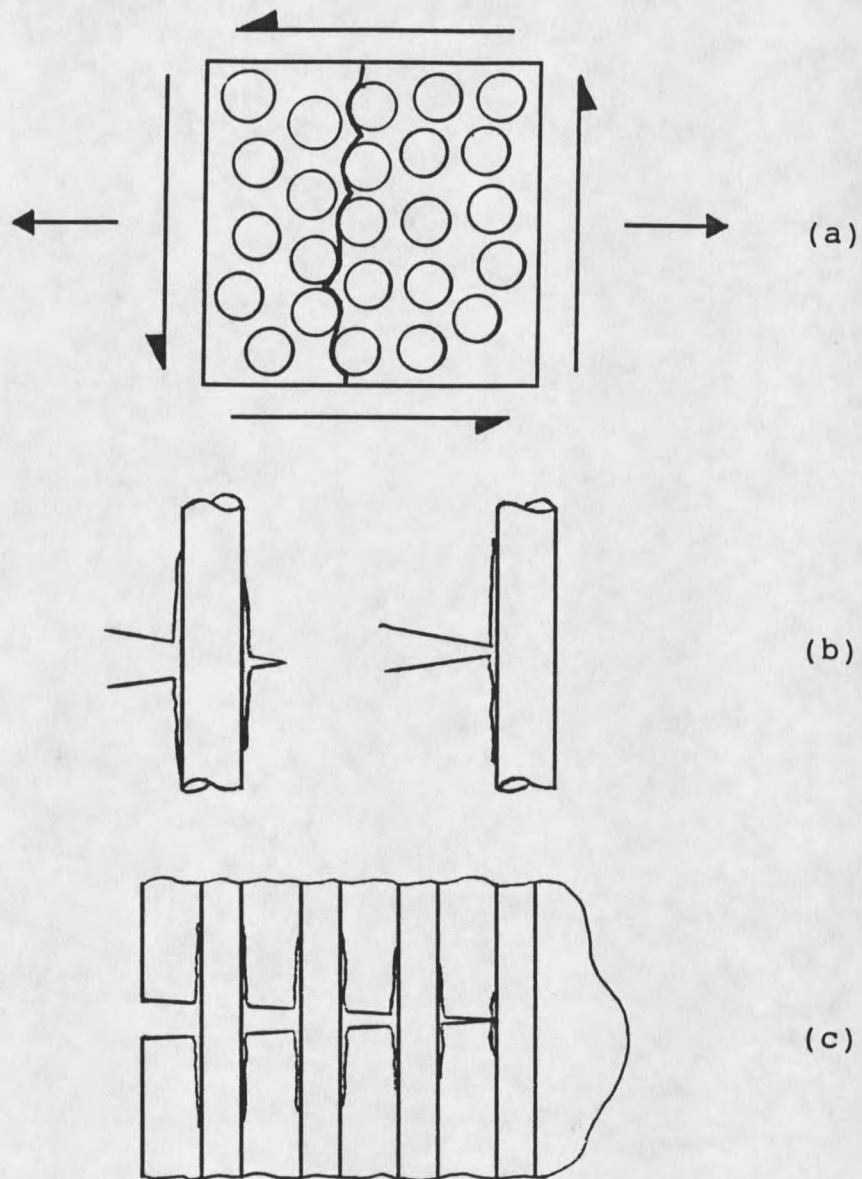


Figure 4. Interface dominated properties [11]: (a) off-axis and shear strength; (b) flaw tolerance (debonding or matrix crack deflection to prevent matrix crack penetration through the fibers); (c) resistance to the growth of matrix cracks in longitudinal tension: propagation of matrix crack with bridging fibers

loaded in tension parallel to the fibers limits their practical use conditions. As described earlier, the opening of large matrix cracks is resisted in part by work done against friction as the matrix slides relative to the unbroken, bridging fibers. Thus, both the tendency to initiate debonding and the subsequent resistance to sliding of the matrix relative to the fibers appear to be two important factors in determining the working stress range of some ceramic matrix materials.

As anticipated, the maintenance of a low interfacial bond strength is critical to achieving composite toughness in the direction of fibers. However, while providing the desired (longitudinal) toughness, this also causes low off-axis composite strength and the need for multiaxial fiber reinforcement for most engineering applications.

Interphase in Nicalon Reinforced Glass-Ceramics

As described earlier, by choosing high-strength, relatively high-modulus, continuous (or relatively long) fibers and incorporating them into matrices, high-strength and tough composites can be created if the fiber-matrix interphase is weak enough to divert and/or bridge cracks. The ultimate strength of such a composite is then controlled by the in-situ fiber strength, and a composite tensile strength well beyond that associated with matrix cracking can be achieved [3]. The

Nicalon-fiber-reinforced lithium-aluminosilicate (LAS) glass-ceramic (Nicalon/LAS) system has met these requirements through the development of a carbon-rich fiber-matrix interphase during processing, and with no deterioration in fiber strength [2,3].

The invention of the continuous polymer-derived SiC based fiber Nicalon (Nippon Carbon Company, Tokyo, Japan) has permitted the development of high-temperature, high-performance ceramic or glass-ceramic matrix composites [2,3,5,20]. Nicalon, with an average tensile strength and elastic modulus of 1920 MPa [21] and 193 GPa [2,20,21] respectively, has a unique nonstoichiometric chemistry that makes it particularly suited to the development of high-strength glass-ceramic matrix composites. Initially, composites with excellent strength were achieved using glass matrices. To achieve the highest levels of temperature resistance, however, the use of crystallized LAS matrices proved most advantageous [2,20]. By densifying (to remove porosity) the composites while the matrix is amorphous and of low viscosity and then crystallizing (ceraming) afterwards, it is possible to produce a very refractory composite with high strength and toughness [2].

Chemical reactions can occur between the fiber and matrix during processing of Nicalon reinforced glass-ceramics, producing the carbon-rich interphase region [3,5,18,20]. The strength of the fiber-matrix interphase and the resulting

composite mechanical properties are significantly influenced by the formation of such interphase regions [18]. The carbon-rich layer of moderate strength effectively limits load transfer between the matrix and the strong fiber either by cohesively failing or adhesively separating from the fiber or the matrix. The carbon-rich layer forms a bond strong enough for load transfer, yet weak enough to debond readily and allow fiber bridging during crack propagation [5,22]. The layer is either nonexistent or carbon-poor in composites that exhibit little toughness [22].

Environmental Effects

Nicalon reinforced glass-ceramic matrix composites with a well developed carbon interphase exhibit excellent longitudinal toughness and crack deflecting ability at room temperature [3,5,20,23]. However, reductions of strength and strain to failure (in the fiber direction) have been observed when testing at temperatures as low as 400°C [24].

The testing of the Nicalon/LAS system in air at 700°C or above has lowered composite tensile strength to the stress level at which matrix cracking begins to occur [25]. Similar embrittlement has been reported for Nicalon/BMAS (barium-magnesium-aluminosilicate) [26] and Nicalon/CAS (calcium-aluminosilicate) [27] composites upon testing in air at temperatures exceeding 800°C. In contrast to room temperature

